Membrane and Cytoskeletal Changes Associated with IgE-mediated Serotonin Release from Rat Basophilic Leukemia Cells

J. R. PFEIFFER,* JC. SEAGRAVE,* B. H. DAVIS,‡ G. G. DEANIN,* and J. M. OLIVER*
Department of Pathology, University of New Mexico School of Medicine, Albuquerque, New Mexico 87131; and ‡Department of Pathology, State University of New York, Upstate Medical Center, Syracuse, New York 13210

ABSTRACT Binding of antigen to IgE-receptor complexes on the surface of RBL-2H3 rat basophilic leukemia cells is the first event leading to the release of cellular serotonin, histamine, and other mediators of allergic, asthmatic, and inflammatory responses. We have used dinitrophenol-conjugated bovine serum albumin (DNP-BSA) as well as the fluorescent antigen, DNP-B-phycoerythrin, and the electron-dense antigen, DNP-BSA-gold, to investigate dynamic membrane and cytoskeletal events associated with the release of [^{3}H]serotonin from anti-DNP-IgE-primed RBL-2H3 cells. These multivalent antigens bind rapidly to cell surface IgE-receptor complexes. Their distribution is initially uniform, but within 2 min DNP-BSA-gold is found in coated pits and is subsequently internalized. Antigen internalization occurs in the presence and absence of extracellular Ca^{2+}. The F-actin content of the detergent-extracted cell matrices analyzed by SDS PAGE decreases during the first 10–30 s of antigen binding and then increases by 1 min to almost double the control levels. A rapid and sustained increase is also observed when total F-actin is quantified by flow cytometry after binding of rhodamine-phalloidin. The antigen-stimulated increase in F-actin coincides with (and may cause) the transformation of the cell surface from a finely microvillous to a highly folded or plicated topography. Other early membrane responses include increased cell spreading and a 2–3-fold increase in the uptake of fluorescein-dextran by fluid pinocytosis. The surface and F-actin changes show the same dependence on DNP-protein concentration as stimulated [^{3}H] serotonin release; and both the membrane responses and the release of mediators are terminated by the addition of the non-cross-linking monovalent ligand, DNP-lysine. These data indicate that the same antigen-stimulated transduction pathway controls both the membrane/cytoskeletal and secretory events. However, the membrane and actin responses to IgE-receptor cross-linking are independent of extracellular Ca^{2+} and are mimicked by phorbol myristate acetate, whereas ligand-dependent mediator release depends on extracellular Ca^{2+} and is mimicked by the Ca^{2+} ionophore A23187.

The release of histamine, serotonin, and other inflammatory mediators from mast cells and basophils is the precipitating event in a variety of acute allergic, asthmatic, and inflammatory reactions (38). This release occurs by the fusion of cytoplasmic granules with each other and with the plasma membrane, leading to the discharge of granule matrix and soluble mediators (13). Current studies of the sequence of biochemical and morphological events leading to degranulation are focused on the rat basophil-like cell line, RBL-2H3 (43). In this cell line degranulation is measured by the release of [^{3}H]serotonin or histamine after cross-linking of surface IgE-receptor complexes with multivalent antigen. Biochemical studies have shown that antigen binding stimulates phosphatidylinositol turnover and generates two second messengers, diacylglycerol to activate protein kinase C and inositol trisphosphate to release Ca^{2+} (2, 3).

We report here our studies of the membrane and cytoskeletal changes associated with IgE-receptor cross-linking on RBL-2H3 cells. A companion paper describes the specific impairment of these responses during mitosis (34). Some of these results have appeared in abstract form (12, 35).

MATERIALS AND METHODS

Cells: The RBL-2H3 cell line developed by Siraganian et al. (43) was a generous gift of Dr. C. Fewtrell, Cornell University. The cells were grown routinely on bacteriological plates in Dulbecco's modified Eagle's medium with 15% fetal calf serum. RBL-2H3 are readily detached from these plates by gentle pipetting or scraping. Cell monolayers were grown on 13-mm glass coverslips in 35-mm bacteriological plates.

Reagents: Mouse monoclonal anti-dinitrophenol IgG (anti-DNP-IgE)[1] (27) was a generous gift from Dr. H. Metzger, National Institutes of Health. Dinitrophenol-conjugated bovine serum albumin (DNP-BSA) and dinitrophenol-conjugated B-phycoerythrin (DNP-PhE) were prepared by Dr. Rosaria Haugland, Molecular Probes, Inc. (Junction City, OR). To ensure maximal release of [^{3}H]serotonin, the conjugates used here had at least 40 DNP substituents per molecule.[2] Gold conjugates (~20-nm diam) of BSA and DNP-BSA were prepared according to Frens (16). Rhodamine-phalloidin (300 U/ml) was from Molecular Probes, Inc.; 5-[1,2-(^{3}H)*N*]-hydroxytryptamine binoxalate ([^{3}H]serotonin; 24.1 Ci/mmol) was from New England Nuclear, Boston, MA; and fluorescein isothiocyanate-conjugated dextran (fluorescein-dextran, 70,000 mol wt) was from Sigma Chemical Co. (St. Louis, MO).

[^{3}H]Serotonin Loading and IgE Labeling: Cells grown on bacterial plates or coverslips were incubated overnight with [^{3}H]serotonin (2 μCi/ml), washed respectively by centrifugation or aspiration, and then incubated for at least 2 h in fresh Dulbecco's modified Eagle's medium with 15% fetal calf serum containing 3 μg/ml anti-DNP-IgE. They were washed into modified Hanks' medium (4) with 0.05% bovine serum albumin (Hanks'-BSA) immediately before use. Except as noted, the Hanks'-BSA contained 1.7 mM Ca^{2+}.

[^{3}H]Serotonin Release: The release of [^{3}H]serotonin from cell suspensions was measured by modification of the procedures of Taurog et al. (45). Cells (0.2 ml; 2×10^6 cells/ml) were added to plastic tubes containing 0.02 ml of either 10 mM HEPES buffer pH 7.4 or an 11× concentration of DNP-protein in 10 mM HEPES buffer. After incubation at 37°C for specified times, the reaction was terminated by addition of 0.5 ml of ice-cold Dulbecco's phosphate-buffered saline (PBS) and a 3-min centrifugation. [^{3}H]Serotonin in 0.5-ml portions of the supernatant was measured by liquid scintillation counting in 4 ml Aquasol. The total serotonin content was determined from the supernatant radioactivity when 0.5% Triton X-100 was added to the cells. Each assay was performed in duplicate or triplicate. Percent [^{3}H]serotonin release was calculated for each condition. Stimulated release was the difference between the percent of total serotonin released in the absence of DNP-protein (spontaneous release) and the percent of total serotonin released in the presence of DNP-protein (spontaneous plus stimulated release).

Cells grown on monolayers were treated similarly except that the coverslips were transferred to 0.2 ml Hanks'-BSA in the 15-mm diameter wells of a 24-well microtiter plate (Costar, Cambridge, MA), followed by addition of 0.02 ml of buffer or DNP-protein to the wells. [^{3}H]Serotonin release was determined by transfer of 0.175 ml of reaction mixture into 0.5 ml ice-cold PBS in 1.5-ml plastic tubes, followed by 3-min centrifugation and liquid scintillation counting of the supernatant fraction. Total radioactivity was again determined from supernatant radioactivity when the cells were treated with 0.5% Triton X-100.

Fluid Pinocytosis: Cells were incubated with fluorescein-dextran (10 mg/ml except as noted) in Hanks'-BSA for various times, then washed once, fixed with 2% paraformaldehyde in PBS for 10 min, washed twice more, and their relative fluorescence intensity and Coulter volume quantified using a Becton-Dickinson FACS analyzer (Becton-Dickinson & Co., Paramus, NJ). In each experiment fluorescence intensity was also measured for a series of standard beads (Becton-Dickinson, Co.). Using the resulting standard curve, mean channel number (log scale) for each sample was converted to mean fluorescence intensity. Further details are given in reference 33.

Electron and Fluorescence Microscopy: For electron microscopic studies, cells were fixed in 2% glutaraldehyde in 0.1 M Na cacodylate pH 7.4 for 30 min at room temperature, rinsed with cacodylate, and processed as described before (11). A Hitachi 600 transmission electron microscope and an ETEC scanning electron microscope (Perkin Elmer-ETEC, Inc., Hayward, CA) were used.

For fluorescence microscopy of fluid and ligand endocytosis, cells were incubated with fluorescein-dextran or DNP-PhE for various times, then fixed with 2% paraformaldehyde in PBS for 10 min, rinsed in PBS, and wet mounted in 50% glycerol in PBS. F-actin labeling was performed by fixing cells for 1 h in 2% paraformaldehyde, followed by 1 h in rhodamine-phalloidin (0.2 ml; 5 U/ml in PBS with 5% methanol) and washing. Cells were observed by epillumination in a Zeiss Photomicroscope III (Carl Zeiss, Inc., Thornwood, NY). They were photographed on Kodak Tri-X-Pan film.

Flow Cytometry: The binding of DNP-PhE to IgE-primed RBL-2H3 cells was measured over time using the facilities of the National Flow Cytometry Resource at Los Alamos National Laboratories, Los Alamos, NM (44). DNP-Phe (1 μg/ml) was added to IgE-primed cell suspensions ($0.5–1.0 \times 10^6$ cells/ml). Simultaneously the ramp generator was activated to provide a time signal (28). The cells were placed in a 37°C sample holder, and fluorescence intensity due to DNP-PhE was measured on a log scale. The cells were excited using the 514-nm line of an argon laser, and fluorescence emission was measured above 540 nm. Data collection was begun within 20–30 s of ligand addition. Results were plotted as DNP-PhE fluorescence against time using the LACEL data reduction programs (40).

The relative amounts of polymerized actin (F-actin) in RBL-2H3 cells were determined by flow cytometry, based on the binding of rhodamine-phalloidin to F-actin in paraformaldehyde-fixed cells. The labeling protocol was modified from Howard and Meyer (22) and Wallace et al. (47). Portions (0.5 ml) of RBL-2H3 ($0.5–1.0 \times 10^6$ cells/ml) were fixed for 1 h with 0.5 ml 4% paraformaldehyde in PBS, pH 7.4, washed with PBS containing 0.1% BSA, then incubated for 1 h in 0.2 ml PBS containing a 1:20 dilution of rhodamine-phalloidin. The suspensions were diluted to 1 ml with PBS-BSA, and the relative fluorescence intensity of the cells was measured on a linear scale using Sorter I at the National Flow Cytometry Resource or a Coulter Epics V flow cytometer at Upstate Medical Center. The cells were excited at 514 nm, and fluorescence emission was measured through 540-nm dichroic and 550-nm-long pass filters. The LACEL programs or the programs of the Coulter MDADS computer were used to derive the mean channels of fluorescence intensity of 10,000 cells.

Preparation and SDS PAGE Analysis of Detergent-extracted Cell Matrices: Cell suspensions (0.22 ml) were incubated for various times with and without DNP-BSA, and then ice-cold 1.5% Triton X-100 in Hanks' medium with 0.1 mg/ml leupeptin (0.4 ml) was added. The suspensions were incubated 5–10 min on ice, then gently layered over 0.8 ml ice-cold 8% sucrose, 1% Triton X-100 in Hanks'-leupeptin without BSA. The tubes were centrifuged for 30 s in an Eppendorf microcentrifuge (13,000 *g*). The supernatant was carefully aspirated, and the pellet was washed with 0.2 ml of the sucrose-Triton-leupeptin solution. The pellets were then suspended in 0.075 ml of a 2× SDS-sample buffer (26) with 50 mM dithiothreitol and incubated at 75°C for 1 h, until solubilized. These extracts were diluted 1:1 with distilled water, and their constituent proteins were separated on 10% SDS polyacrylamide gels with 3% acrylamide stacking gels by the procedure of Laemmli (26). Molecular weight and actin standards were included in each gel.

The relative intensities of protein bands were determined by scanning the Coomassie Blue-stained gels with a Zeineh soft laser densitometer (BioMed Instruments, Inc., Fullerton, CA). Analysis of actin standards established that the peak heights of the densitometer tracings of actin were linear with concentrations over the range observed.

RESULTS

Kinetics of [^{3}H]Serotonin Release

Fig. 1*A* shows time courses of antigen-stimulated [^{3}H]-serotonin release from anti-DNP-IgE-primed RBL-2H3 cell suspensions and cell monolayers. [^{3}H]Serotonin release is detected at 1 min after addition of 1 μg/ml DNP-protein to cell suspensions and continues at a linear rate for ~20 min. Release may be initiated in <1 min; however, our assay does not show significant differences between spontaneous and stimulated release at very early times. The kinetics of release

[1] *Abbreviations used in this paper:* anti-DNP-IgE, anti-dinitrophenol IgE; DNP-BSA, dinitrophenol-conjugated bovine serum albumin; DNP-PhE, dinitrophenol-conjugated B-phycoerythrin; fluorescein-dextran, fluorescein isothiocyanate-conjugated dextran; Hanks'-BSA, modified Hanks' medium with 0.05% bovine serum albumin; PMA, phorbol myristate acetate.

[2] Seagrave, J. C., G. G. Deanin, J. Martin, B. H. Davis, and J. M. Oliver. Manuscript submitted for publication.

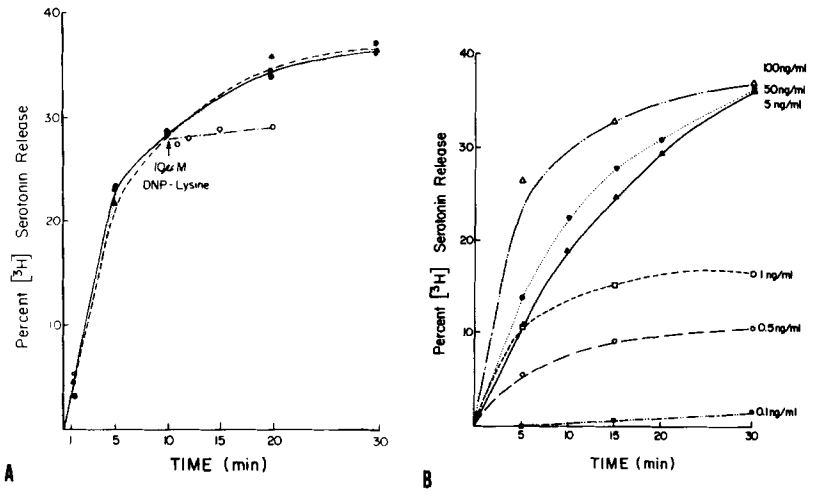

FIGURE 1 The time course (*A*) and concentration dependence (*B*) of DNP-protein-stimulated [^{3}H]-serotonin release from RBL-2H3 cells. In *A*, [^{3}H]-serotonin release was measured in anti-DNP-IgE-primed cells incubated in suspension with 1 μg/ml DNP-BSA (●), or with 1 μg/ml DNP-PhE (▲); and in cell monolayers incubated with 1 μg/ml DNP-BSA (□). Addition of DNP-lysine (10 μM; arrow) to DNP-BSA-treated cells abruptly terminates [^{3}H]-serotonin release (○). In *B*, [^{3}H]serotonin release was measured in anti-DNP-IgE-primed cells incubated with DNP-BSA between 0.1 and 100 ng/ml. Curve fitting was performed using the method of least squares.

are essentially identical when cell suspensions are stimulated by 1 μg/ml DNP-PhE and when DNP-BSA is added to cell monolayers. A 1:100 dilution of the 20 nm DNP-BSA-gold particles also induced maximum [^{3}H]serotonin release (data not shown). Addition of an excess of the monovalent, competitive ligand, DNP-lysine prevents further binding of polyvalent ligand (25) and terminates degranulation.

Fig. 1*B* shows the kinetics of [^{3}H]serotonin release as a function of DNP-BSA concentration. [^{3}H]Serotonin release is maximal at or above 5 ng/ml DNP-BSA. At lower concentrations there is a decline in both the rate and extent of mediator release. Nevertheless, stimulated [^{3}H]serotonin release is detectable to concentrations as low as 0.5 ng/ml DNP-BSA. Similar results were obtained with the fluorescent conjugate, DNP-PhE, except that maximum release requires at least 50 ng/ml DNP-PhE, and no release occurs at concentrations below 5 ng/ml DNP-PhE.[2]

Other investigators have reported that essentially no release of [^{3}H]serotonin occurs from IgE-primed cells incubated with antigen in medium lacking Ca^{2+}, with or without the addition of EGTA, and that the Ca^{2+} ionophore A23187 in the presence of Ca^{2+} directly stimulates the release of [^{3}H]serotonin (15, 45). The same results were obtained in our laboratory (data not shown).

In rat mast cells, phorbol esters such as phorbol myristate acetate (PMA) do not stimulate mediator release even though they potentiate A23187-induced release (20). Similarly we find no stimulation of [^{3}H]serotonin release from RBL-2H3 cells incubated with PMA at concentrations between 1 and 100 nM (data not shown).

Kinetics of Ligand–IgE–Receptor Binding

The binding of DNP-PhE and DNP-BSA-gold was measured respectively by flow cytometry and by counting gold particles in the electron microscope. In both cases the cross-linker concentration used causes maximal [^{3}H]serotonin release. Fig. 2 shows the kinetics of DNP-PhE (1 μg/ml) binding to untreated and IgE-primed RBL cells. This binding measurement is made in the continuous presence of the ligand. There is no binding to cells lacking cell surface IgE; essentially all IgE-primed cells bind DNP-PhE, and maximum binding is achieved in <1 min. The kinetics of binding are the same in the presence or absence of Ca^{2+} (data not shown).

In apparent contrast with the flow cytometry data, the

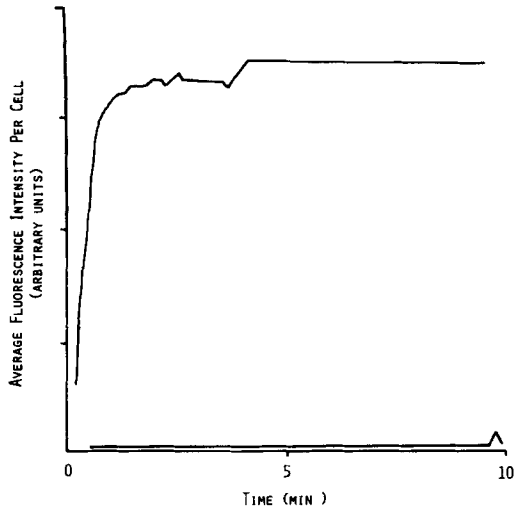

FIGURE 2 The time course of DNP-PhE binding to IgE-receptor complexes. DNP-PhE (1 μg/ml) binds rapidly to IgE-primed cells (upper curve). There is no binding to cells without surface IgE (lower curve).

DNP-BSA-gold particles show a progressive increase in binding to cells over a 2–10-min period (Table I). In this analysis, cells were washed after labeling with antigen. A progressive increase in binding was also observed when cells were labeled with DNP-PhE (1 μg/ml), then fixed and washed before analysis by flow cytometry (not shown). We postulate that an initial rapid but readily reversible binding event (measured only in the continuous presence of ligand) is followed by a less reversible binding process (measured in washed cells). These kinetic observations are explored further in a separate report.[2]

Distribution and Mobility of Ligand–IgE–Receptor Complexes

The fluorescence micrographs in Fig. 3 show the progression of DNP-PhE (1 μg/ml) from a uniform distribution at 4°C (*A*), into a patchy distribution on the cell surface by 1 min at 37°C (*B*), and into cytoplasmic vesicles by 10 min at 37°C (*C*). The same rapid internalization of DNP-PhE was observed by fluorescence microscopy of cells incubated with antigen in the presence or absence of extracellular Ca^{2+}. The Ca^{2+}-independence of antigen uptake has been confirmed by

TABLE I. *Binding and Distribution of Gold Conjugates on RBL-2H3 Cells*

Gold conjugates	Labeling conditions	Total gold particles/20 cells	Particles on the cell surface	Surface-bound particles in coated pits	Coated pits/20 cells
			%	%	
BSA-gold	5 min, 37°C	13	100	0	108
DNP-BSA-gold	20 min, 4°C	638	97	5	—
DNP-BSA-gold	0.05% glutaraldehyde (10 min), then 5 min, 37°C	97	100	0	—
DNP-BSA-gold	2 min, 37°C	332	86	26	109
DNP-BSA-gold	5 min, 37°C	708	47	33	100
DNP-BSA-gold	10 min, 37°C	1,262	36	19	101

All cells were incubated with anti-DNP-IgE before labeling with 20 nm-diam gold conjugates (1:100 dilution). 20 cells were selected at random for each condition and examined for their total number and distribution of BSA-gold (control) and DNP-BSA-gold (experimental) particles. In most samples the total number of coated pits per cell was also recorded.

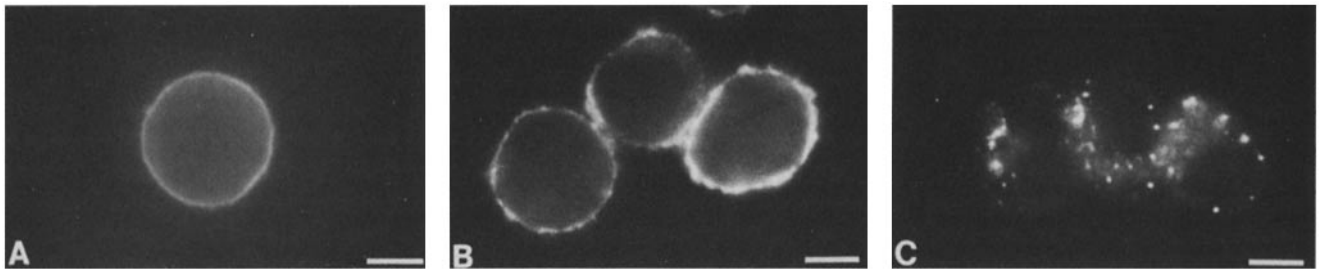

FIGURE 3 The distribution and internalization of cross-linked IgE-receptor complexes: fluorescence microscopy. Anti-DNP-IgE-treated RBL-2H3 were incubated with 1 μg/ml DNP-PhE for 10 min at 4°C (*A*); or at 37°C for 1 min (*B*) and 5 min (*C*). Bar, 5 μm.

flow cytometry of cells incubated for various times with antigen followed by DNP-lysine to displace most of the surface-bound DNP-PhE.[2]

This sequence of events is revealed in detail by electron microscopy (Table I and Fig. 4). On cells labeled at 4°C or after light fixation (0.05% glutaraldehyde, 10 min) essentially all the gold particles are on the cell surface and <5% of these particles are associated with coated pits. After labeling at 37°C for 2 min, the majority of DNP-BSA-gold particles are still on the cell surface (Fig. 4*A*). However, 26% of particles are now associated with coated pits or vesicles. An average of 26% of the surface-associated particles are also in coated pits when cells are incubated with ligand at 37°C for 5 or 10 min. However after 5 min, almost half of the gold particles are located in intracellular, smooth vesicles near the plasma membrane (Fig. 4*B*), and after 10 min, >60% of the gold particles are located in intracellular smooth vesicles that concentrate in the region of the Golgi complex (Fig. 4*C*). The number of coated pits per cell remains constant throughout the process of ligand redistribution and internalization (Table I).

Surface Topography

DNP-protein causes a remarkable transformation in RBL-2H3 cell surface topography. Whereas control cells maintain a finely microvillous cell surface (Fig. 5*A*), essentially every cell incubated with DNP-BSA develops a series of broad membrane ridges (plicae, lamellipodia) that form an intersecting, often honeycomb-like pattern on the cell surface. This transformation occurs very quickly. Ridges are visible on cells exposed to DNP-BSA (1 μg/ml) for only 30 s (Fig. 5*B*) and the maximal response, characterized by a honeycombed morphology, is apparent by 5 min (Fig. 5*C*). This transformation requires the continued occupation of cell surface receptors by multivalent antigen. The ridges regress within 2 min after addition of DNP-lysine (Fig. 5*E*), and reversal of the surface transformation is essentially complete after 5 min (Fig. 5*F*).

The extent of surface transformation varies with DNP-BSA concentration. The lowest concentration that induces the surface change is 0.5 ng/ml DNP-BSA (Fig. 6*B*). Surface stimulation is more clearly evident at 1 ng/ml DNP-BSA

FIGURE 4 The distribution and internalization of cross-linked IgE-receptor complexes: electron microscopy. Anti-DNP-IgE-treated RBL-2H3 were incubated with 20 nm DNP-BSA-gold particles (1:100 dilution) at 37°C for 2, 5, and 10 min. Cells labeled for only 2 min (*A*) show little if any internalization. However a high proportion of surface-associated particles are in coated pits (arrows; see inset of *A*). There is a progressive redistribution with time of gold particles (circles) from the cell surface, first to cytoplasmic smooth vesicles near the cell surface (*B*) and then to smooth vesicles that accumulate in the region of the Golgi stacks (C). Bars, 0.5 μm. Bar of inset, 0.1 μm.

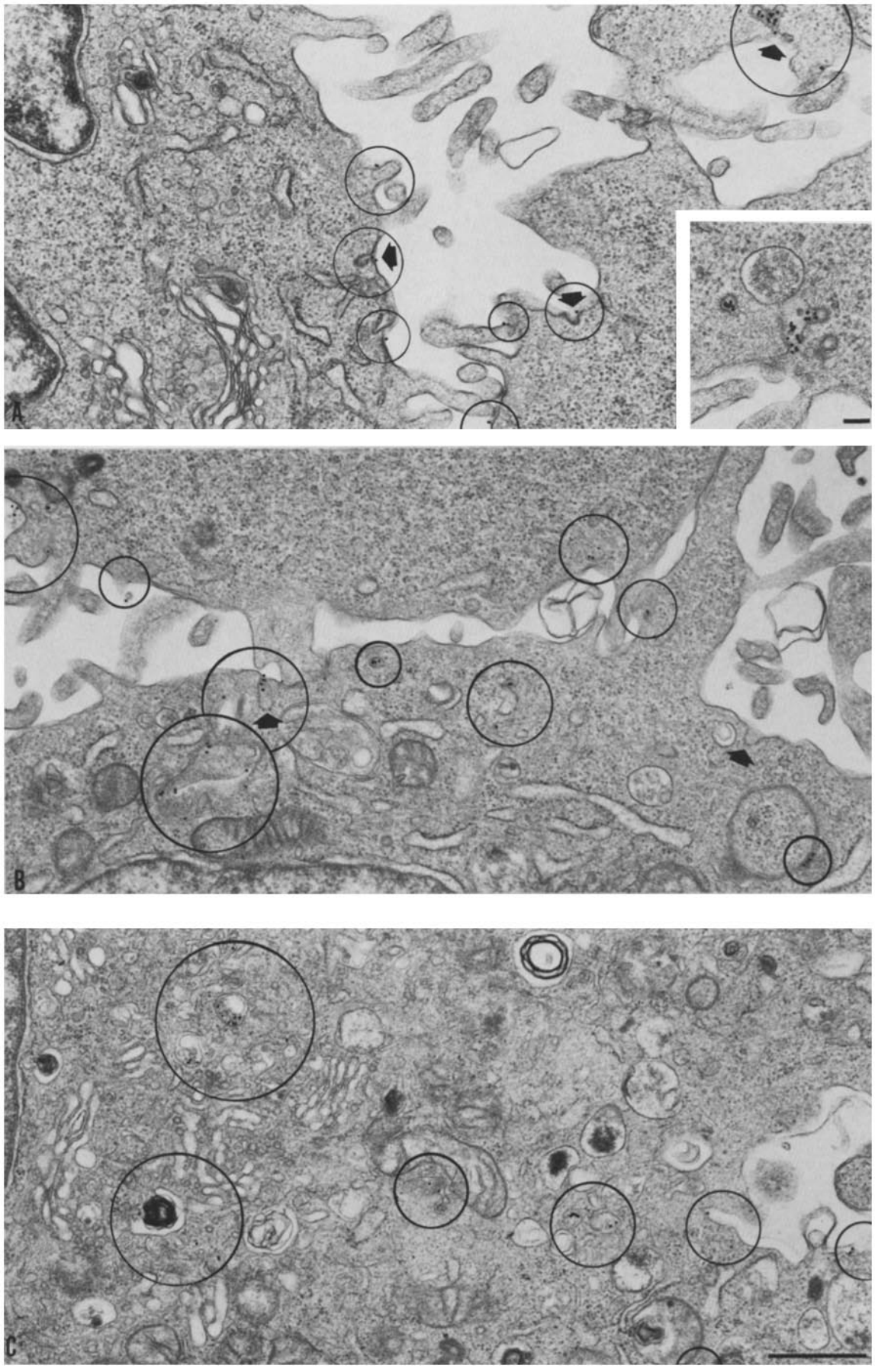
A
B
C

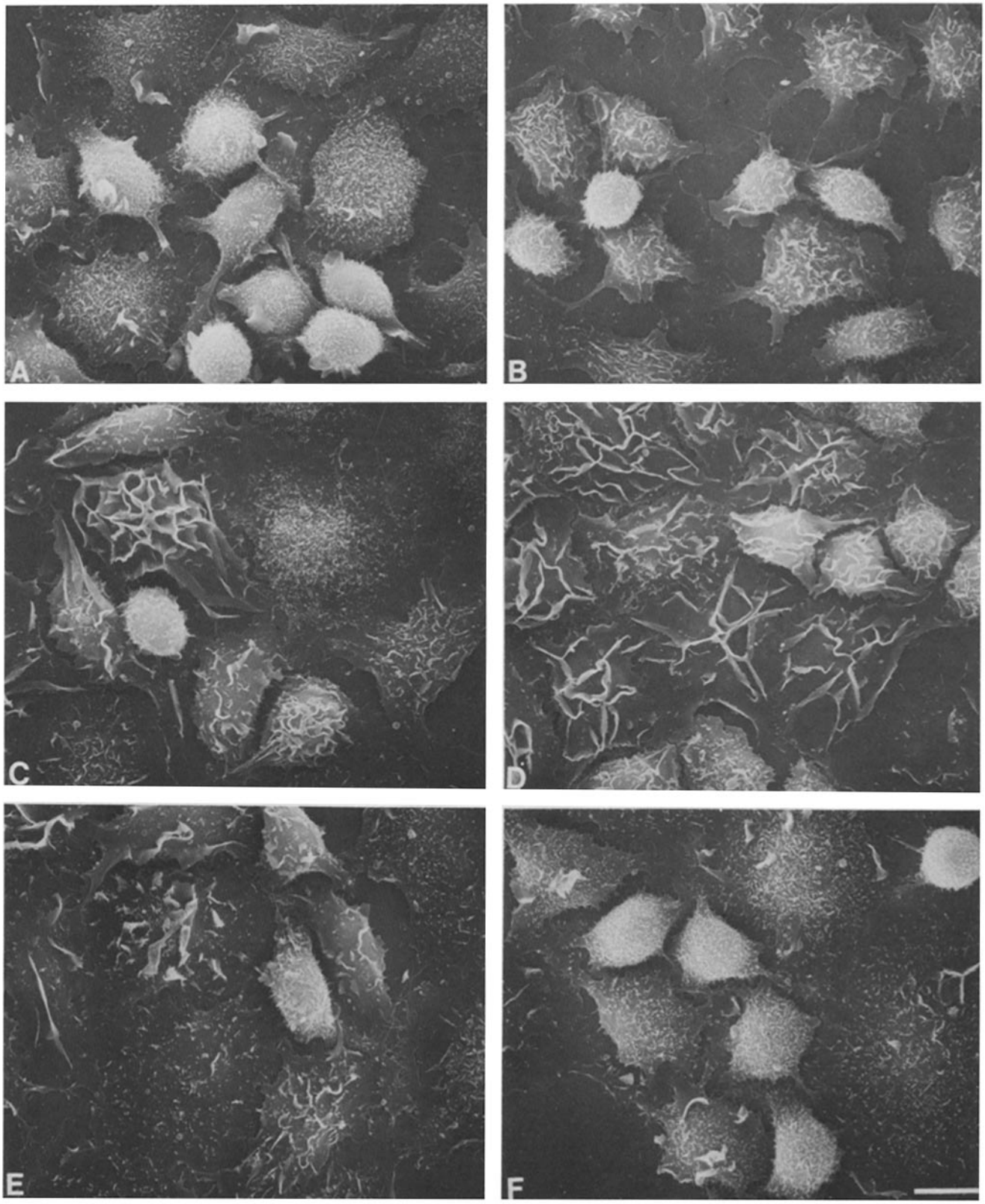

FIGURE 5 The induction and reversal of surface transformation after IgE-receptor cross-linking. The microvillous surface topography of cells incubated with IgE alone is shown in *A*. The cells were stimulated with 1 μg /ml DNP-BSA for 0.5 min (*B*), 5 min (*C*), or 10 min (*D*). The development of broad membrane folds or plicae and increased cell spreading are detectable at 0.5 min and maximal by 5 min. Surface topography was reversed from plicated to microvillous by exposing cells to 1 μg/ml DNP-BSA for 10 min, followed by incubation with 10 μm DNP-lysine for 2 min (*E*) or 5 min (*F*). Bar, 10 μm.

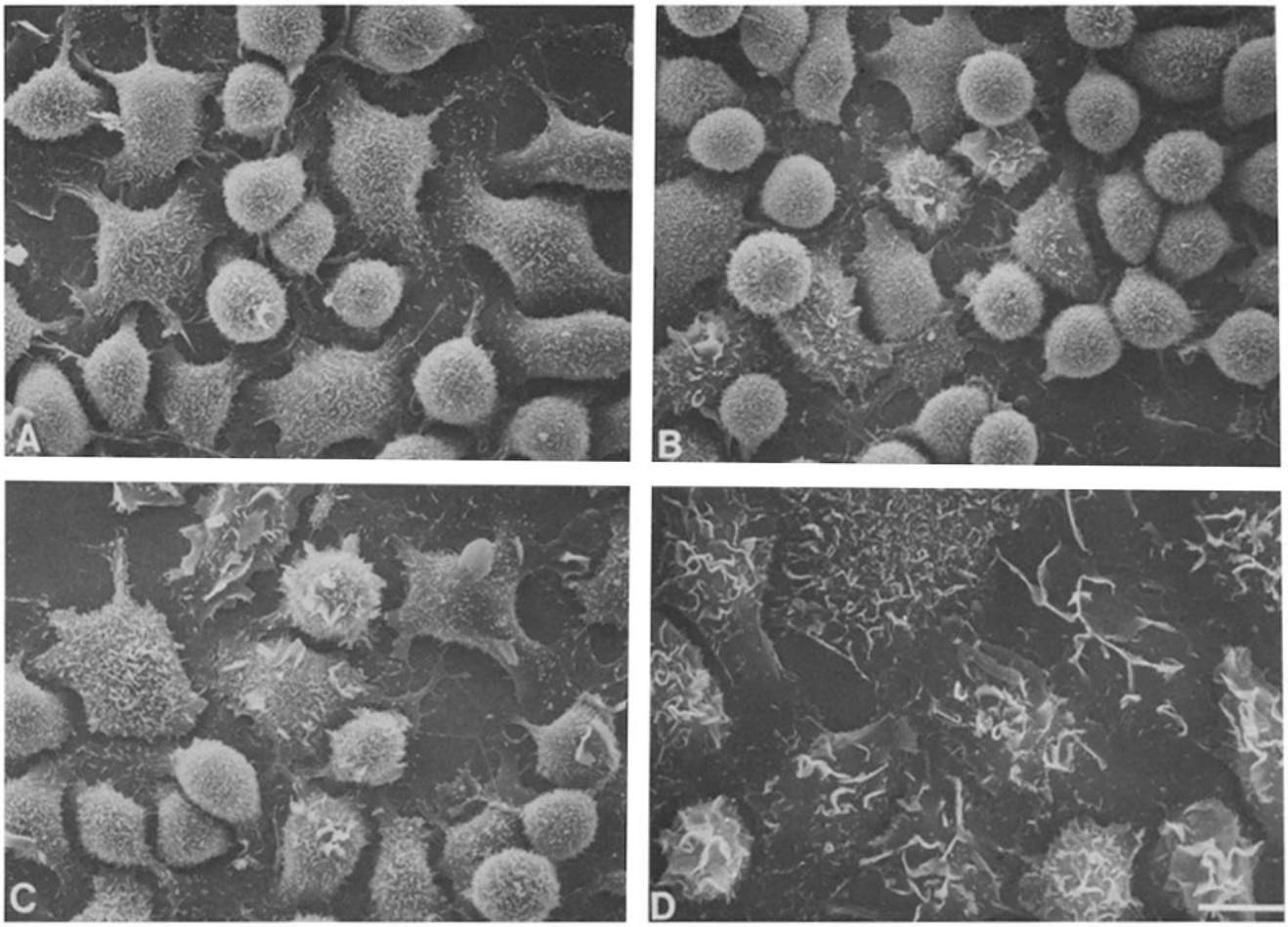

FIGURE 6 The effect of varying DNP-BSA concentrations on surface transformation. Anti-DNP-IgE-primed RBL-2H3 cells were incubated for 15 min at 37°C with Hanks'-BSA containing DNP-BSA at 0.1 ng/ml (*A*); 0.5 ng/ml (*B*); 1 ng/ml (*C*); and 5 ng/ml (*D*). Bar, 10 μm.

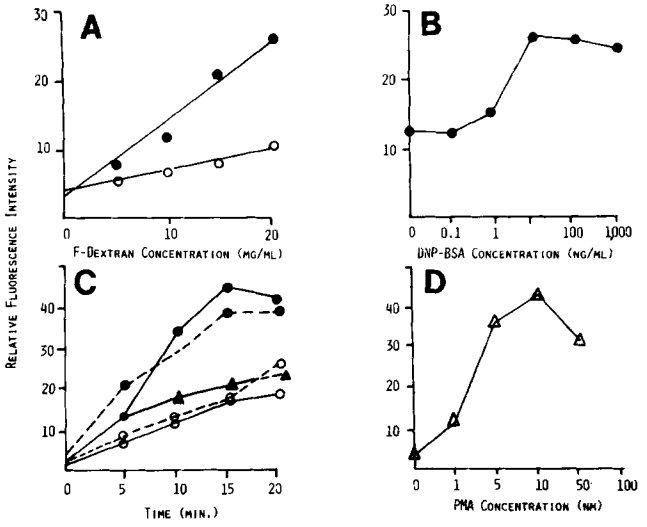

FIGURE 7 Quantitation of fluorescein-dextran uptake after IgE-receptor cross-linking. *A* shows there is a linear relationship between fluorescein-dextran concentration in the medium and its uptake into control (lower line) and DNP-BSA (1 μg/ml) treated (upper line) RBL-2H3 cells over 20 min. *B* shows that the uptake of fluorescein-dextran by anti-DNP-IgE-primed cells during a 20-min incubation is stimulated at all concentrations of DNP-BSA above 1 ng/ml. *C* shows the time course of fluorescein-dextran uptake (10 mg/ml) for anti-DNP-IgE-primed cells incubated with buffer alone (○), and with 1 μg/ml DNP-BSA (●). Uptake is essentially the same in the presence (——) or absence (– – –) of Ca^{2+}. The stimulated uptake of fluorescein-dextran is inhibited by the addition after 5 min of 10 μM DNP-lysine (▲). *D* shows that a dose-dependent increase in fluid pinocytosis occurs when cells are incubated in Hanks'-BSA with concentrations of PMA between 1 and 10 nM. The stimulation of pinocytosis is reduced at higher PMA concentrations.

(Fig. 6*C*), and the maximum response is seen at and above 5 μg ng/ml DNP-BSA (Fig. 6*D*).

Further scanning electron microscopic analyses (not illustrated here) established that the transformation of surface topography from microvillous to plicated is completely independent of the presence of Ca^{2+} in the incubation medium. It was also shown that 1 nM PMA was sufficient to cause moderate ruffling and that 10 nM PMA caused the same surface transformation as occurred in response to 1 μg/ml DNP-protein. PMA-induced ruffling is illustrated in the companion paper (34). The Ca^{2+} ionophore A23187 caused no ruffling when added to cell monolayers in medium lacking Ca^{2+} or in medium containing between 10 μM and 1.7 mM Ca^{2+}.

Cell Spreading

The scanning electron micrographs show that IgE-receptor

cross-linking causes a dramatic increase in cell spreading. This response is evident in cells incubated for 30 s with 1 μg/ml DNP-BSA (compare Figs. 5, *A* and *B*) and is maximum by 5–10 min (Figs. 5*D* and 6*D*). It occurs at concentrations as low as 1 ng/ml DNP–BSA (compare Fig. 6*A* with 6*C*).

Fluid Pinocytosis

Unstimulated RBL-2H3 cells internalize fluorescein–dextran by a process that is linear with fluorescein–dextran concentration and with time (Fig. 7, *A* and *C*, lower curves). These are the kinetics predicted for fluorescein–dextran uptake by fluid pinocytosis (33). IgE–receptor cross-linking induces a rapid stimulation of this uptake process. Thus, DNP–BSA (1 μg/ml) increases the amount of fluorescein ingested in 10 min by 2–3-fold (Fig. 7*A*), and it increases the rate of fluorescein–dextran uptake, at least over 15 min (Fig. 7*C*). The antigen-induced stimulation of fluorescein–dextran uptake shows the same ligand concentration-dependence as [^{3}H]serotonin release (Fig. 7*B*); it occurs whether or not the incubation medium contains Ca^{2+} (Fig. 7*C*) and is terminated by the addition of DNP–lysine (Fig. 7*C*). A23187 does not stimulate fluid uptake (data not shown), but PMA increases pinocytosis over a concentration range of 1–10 nM. Fluid uptake declines at 50 nM and higher concentrations of PMA (Fig. 7*D*). Fluorescence micrographs of the distribution of fluorescein–dextran in control and stimulated cells are given in the companion paper (34).

F-Actin Content of RBL-2H3 Cells

The SDS polyacrylamide gel in Fig. 8 shows the effect of IgE–receptor cross-linking on the major proteins of the RBL-2H3 cell matrix. A band that co-migrates with actin is prominent in both untreated and antigen-stimulated RBL-2H3 cells. The intensity of this band is reduced during the first seconds after addition of DNP–BSA to cells and is increased during the subsequent 1–10 min.

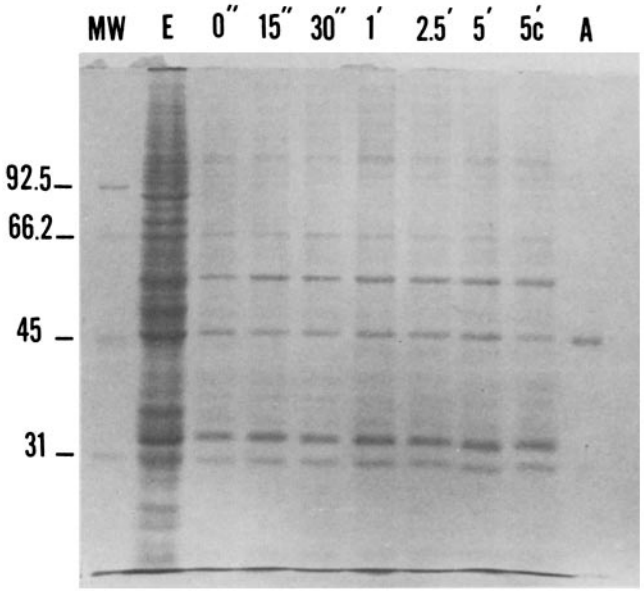

FIGURE 8 SDS PAGE analysis of RBL-2H3 Triton-insoluble matrices. Triton X-100 extracts were prepared after incubation of 5 × 10^6 cells for various times with DNP–BSA (1 μg/ml) in medium containing Ca^{2+}. The extracts were separated by SDS PAGE on 10% polyacrylamide gels. The first two lanes show molecular weight markers (*MW*) and whole cell extract (*E*), respectively. The last lane contains only authentic actin (*A*). The intermediate lanes show the proteins remaining after detergent extraction of cells that were incubated with antigen for increasing times (marked in seconds and minutes). The cells in the lane marked 5C were incubated in Hanks'–BSA alone for 5 min before extraction.

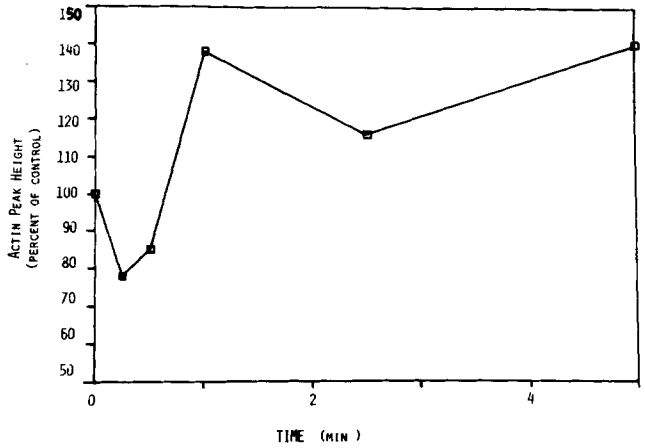

FIGURE 9 Quantification of actin as a function of IgE–receptor cross-linking. The actin peak heights taken from densitometric traces of the gel in Fig. 8 were plotted against time. This typical experiment shows an initial decrease and later increase in actin associated with matrices prepared from antigen-stimulated cells.

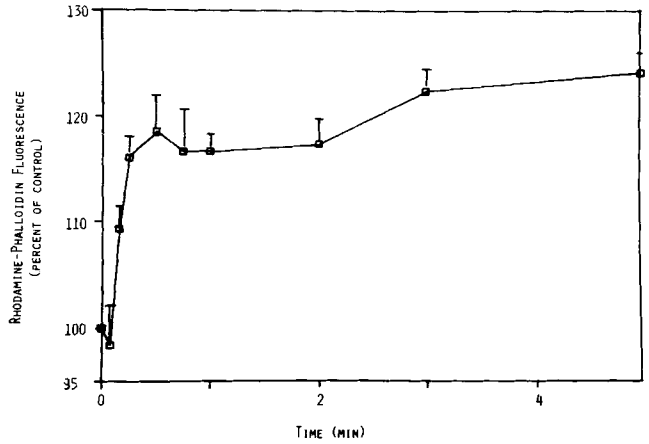

FIGURE 10 Quantification of rhodamine–phalloidin binding to RBL-2H3 cells. RBL-2H3 cells were incubated with DNP–BSA (1 μg/ml) for the times indicated, then fixed, and F-actin was labeled with rhodamine–phalloidin. Results are the mean ± SD for four separate experiments. The F-actin content continued to increase slowly beyond 5 min, reaching a maximum of 31.5 ± 2.6% above control after 15 min.

The kinetics of the sequential drop and increase in F-actin content of detergent-extracted cell matrices was established by densitometric analysis of this and similar gels. Fig. 9 shows that the relative actin content of the detergent-extracted matrices decreases over the first 30 s after addition of DNP–BSA (1 μg/ml). The actin content subsequently increases to almost twice the control level. Qualitatively similar results were obtained in replicate experiments performed in the presence and absence of Ca^{2+}. Thus, in four separate analyses in medium containing Ca^{2+} and in two additional analyses without Ca^{2+}, the minimum F-actin content, reached at times varying from 10 to 30 s after addition of DNP–BSA (1 μg/ml), was 25.00% ± 14.4% (SD) below the corresponding control values. In

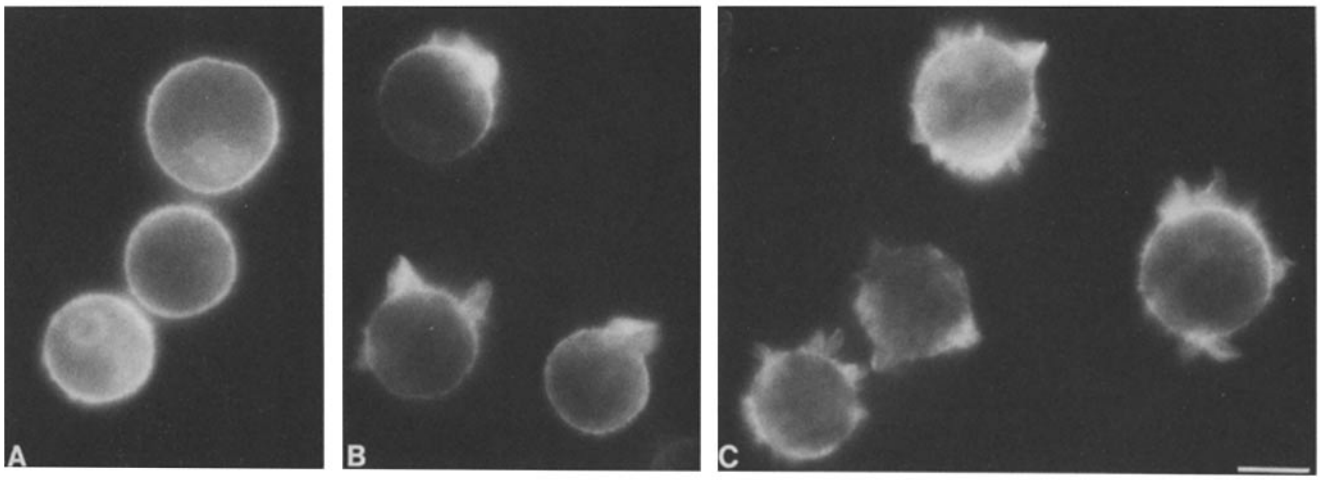

FIGURE 11 The distribution of rhodamine-phalloidin in resting and stimulated RBL-2H3 cells. IgE-primed cells were exposed to DNP-BSA (1 μg/ml) for 0 min (*A*), 5 min (*B*), and 10 min (*C*) then fixed and their F-actin labeled with rhodamine-phalloidin. The transformation of surface topography from microvillous to plicated is illustrated. Bar, 10 μm.

eight analyses, three performed without Ca^{2+}, the maximum F-actin content, reached between 1 and 5 min after addition of antigen, was 78.4% ± 30.84% (SD) above the corresponding control values. The Ca^{2+} ionophore A23187 (0.4 μM) had no consistent effect on the actin content of matrices prepared from RBL-2H3 cells incubated between 15 s and 15 min in medium without Ca^{2+} or with 1.7 mM Ca^{2+} (data not shown).

Flow cytometric analysis of F-actin content based on the binding of rhodamine-phalloidin revealed a similar but not identical pattern of reorganization. Fig. 10 shows the average fluorescence intensity measured in four separate experiments. An initial lag during the first seconds of stimulation was followed by an abrupt increase to ~1 min, then a plateau and a further gradual increase in cellular fluorescence. The final level of fluorescence, which was 31.5% ± 2.6% (SD) above the control level, was reached after 15 min. The fluorescence due to rhodamine-phalloidin outlined the surface lamellae of the stimulated cells, indicating that the F-actin-phalloidin complexes were associated to a large extent with the plasma membrane (Fig. 11).

We confirmed by flow cytometry that the increase in F-actin varies as a function of DNP-protein concentration (Fig. 12) and is independent of extracellular Ca^{2+} (data not shown). By analyzing fluorescence intensity as a function of Coulter volume, we also established that the shift in rhodamine-phalloidin fluorescence intensity occurs in all cells and not simply in a subpopulation of cells.

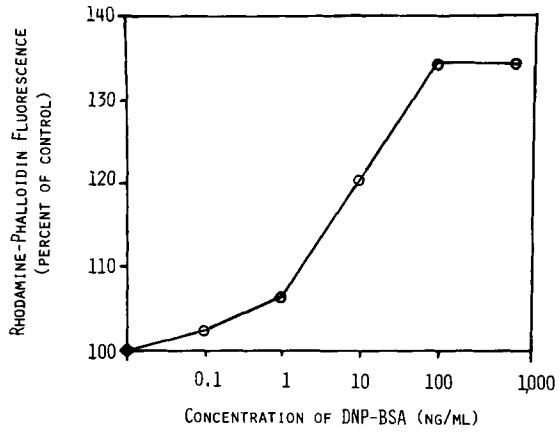

FIGURE 12 The binding of rhodamine-phalloidin increases with DNP-BSA concentration. IgE-primed cells were incubated for 15 min with DNP-BSA at concentrations between 1 ng/ml and 1 μg/ml. A dose-dependent increase in fluorescence intensity was observed.

DISCUSSION

The receptor for IgE is univalent, mobile, and uniformly distributed on the RBL-2H3 cell surface (29, 30). It has been established that limited receptor cross-linking is adequate to stimulate mediator release (14), and it is known that localized aggregation is followed by the clustering and internalization of cross-linked IgE-receptor complexes (31). The receptor has been purified from RBL-2H3 cells and characterized by Metzger and colleagues (21, 39).

We show here that antigen binds rapidly to IgE-receptor complexes and that the resulting complexes redistribute into coated pits on the cell surface. About 25% of the surface-associated DNP-BSA-gold particles are in pits within 2 min of ligand binding, and this same high proportion of particles bound to pits is maintained after 5 and 10 min of incubation. Thus a continuous process of antigen binding and redistribution to coated pits occurs during the period of antigen-stimulated [^{3}H]serotonin release. Internalization follows redistribution, and the gold particles eventually accumulate in the peri-Golgi region of the cell. Cells incubated with antigen in the absence of extracellular Ca^{2+} internalize antigen-IgE-receptor complexes at the same rate as cells incubated in medium with Ca^{2+}. However no mediator release occurs in Ca^{2+}-free medium. We postulate that the progressive loss of degranulation competence (desensitization) that occurs when RBL-2H3 cells are incubated with antigen in Ca^{2+}-free medium (2) results in part from this Ca^{2+}-independent removal of antigen-IgE-receptors from the cell surface. Furuichi et al. (17) have advanced a similar hypothesis.

We obtained no evidence for long-range movement of ligand-IgE-receptors into surface caps. This result is different from Carson and Metzger's (6) evidence for capping but not internalization of complexes between IgE-receptor complexes and fluorescein-anti-IgE. However these investigators studied the parental RBL-1 line that does not release mediators after

cross-linking of IgE–receptor complexes. More recently several groups have reported that fluorescent multimeric IgE, as well as radiolabeled DNP–proteins, are rapidly internalized and rarely capped on RBL-2H3 cells (17, 23, 31).

A series of dynamic changes in the cell surface and cytoskeleton of RBL-2H3 cells accompanies the cross-linking and redistribution of anti–DNP-IgE-receptor complexes. The most dramatic membrane response is the transformation of cell surface topography from a microvillous appearance to a highly plicated appearance. This transformation is apparent within 30 s of DNP–protein addition to anti–DNP-IgE–treated cells, it persists through the entire period of degranulation, and the plicae regress rapidly after addition of the monovalent ligand, DNP–lysine, that prevents further binding of multivalent antigen. Surface transformation can be detected on cells exposed to DNP–BSA concentrations at the lower limits for stimulated release of [^{3}H]serotonin. The transformation of surface topography is associated with increased cell spreading and with a 2–3-fold increase in the rate of fluorescein–dextran uptake by fluid pinocytosis.

IgE–receptor cross-linking also results in dramatic changes in the actin content of detergent-extracted RBL-2H3 cell matrices. Antigen binding causes a decrease in the actin content of detergent-extracted matrices to 25% below control levels. The decrease occurs during the first 10–30 s of stimulation and thus precedes the membrane responses. It is followed between 30–60 s by an increase to almost twice that of control levels. This increase is sustained for at least 20–30 min. Flow cytometric analyses of rhodamine-phalloidin–labeled cells confirm the sustained increase in F-actin content of stimulated cells and establish that the increase can be detected at the lowest concentrations of DNP–protein that stimulate [^{3}H]serotonin release. Fluorescence microscopy of the rhodamine-phalloidin–labeled cells indicates that much of the F-actin is localized to the surface plicae or lamellipodia that form in response to IgE–receptor cross-linking.

The flow cytometric analysis does not show the dramatic initial decrease in F-actin content that is revealed by SDS PAGE analysis of detergent-insoluble matrices. This difference, as well as the smaller overall increase in F-actin measured by the fluorescence analysis, may reflect the somewhat different parameters measured by the two techniques. The fluorescence method reflects the total F-actin content of the cells, whereas the SDS PAGE analysis is weighted towards membrane-associated actin. Thus, if a proportion of the F-actin remains polymerized but is dissociated from the plasma membrane during the initial 10–30 s of stimulation, it might be included in the analysis of total F-actin but might not appear in the analysis of membrane-associated F-actin. Similarly the majority of the newly polymerized actin may be membrane-associated, yielding a higher final increase in F-actin by SDS PAGE analysis of detergent-insoluble matrices than by fluorescence analysis of rhodamine–phalloidin binding. Of course different rates of F-actin stabilization or fixation by the two methods could also be involved.

What is the relationship of these membrane and cytoskeletal responses to the process of degranulation? We show here that the ligand concentration dependence of ruffling, pinocytosis, and increased actin assembly exactly parallels the ligand concentration dependence of [^{3}H]serotonin release. Furthermore both the membrane changes and mediator release are rapidly terminated by the monovalent competitive ligand, DNP-lysine. These data indicate that the same antigen-stimulated transduction pathway controls both the membrane responses and the release of mediators. On the other hand, the membrane and cytoskeletal events can be dissociated from degranulation based on their different responses to drug treatment. Thus antigen-stimulated mediator release depends on extracellular Ca^{2+} and the ionophore A23187 plus Ca^{2+} can substitute for ligand in causing the release reaction. In contrast ligand-stimulated ruffling, fluid pinocytosis, IgE–receptor internalization, and actin assembly all occur in the absence of extracellular Ca^{2+}, and A23187 plus Ca^{2+} elicits no membrane or cytoskeletal responses. Furthermore, PMA, the tumor promoter that activates protein kinase C, stimulates ruffling, spreading, and fluid pinocytosis without inducing [^{3}H]serotonin release.

It now appears that the specific responses of a range of target cells to appropriate hormones, growth factors, and immune mediators begin with the activation of a GTP binding protein(s) (8) that in turn stimulates phospholipase C and leads to the increased hydrolysis of phosphatidylinositol 4,5-bisphosphate (32). Phosphatidylinositol 4,5-bisphosphate hydrolysis leads to the generation of diacylglycerol that activates protein kinase C and to the formation of inositol trisphosphate that may mobilize cytoplasmic Ca^{2+} stores. Cross-linking of IgE–receptors with antigen stimulates inositol phospholipid turnover and also promotes the uptake of extracellular Ca^{2+} by RBL-2H3 cells (2, 3). We postulate that the common event leading to membrane/cytoskeletal responses and mediator release may be the activation of a GTP binding protein and the resulting increase in phospholipase C activity and Ca^{2+} influx. Mediator release may depend most importantly on the mobilization of Ca^{2+}, while the membrane and cytoskeletal responses may depend principally on the activation of protein kinase C.

This pharmacological dissociation indicates that membrane and cytoskeletal reorganization is not an essential component of the final degranulation pathway. Nevertheless the membrane/cytoskeletal responses may modulate the ligand-stimulated triggering of the Ca^{2+}-dependent release pathway. Thus, Vale and Shooter (46) and others (24, 41) have suggested that the interaction of cortical actin with receptors or other membrane proteins can modulate the kinetics of ligand–receptor interaction and may thereby modulate specific cellular responses. In neutrophils and lymphocytes, this modulation is thought to be associated with the actin-dependent stabilization of receptors against detergent extraction (24, 48). A similar stabilization may occur in RBL-2H3 cells; recently Baird et al. (1) reported an increased association of the IgE–receptor with RBL-2H3 detergent-insoluble matrices after cross-linking with IgE multimers. The significance of the transient decrease in membrane-linked actin, which precedes the membrane responses, is presently unknown.

A very similar series of membrane responses follows interaction of a range of hormones, mitogens, and immune mediators with their receptors. For example increased membrane ruffling, fluid pinocytosis, and/or cell spreading are common, as well as early responses to the binding of nerve growth factor, epidermal growth factor, insulin, and melanocyte-stimulating hormone to target tissues (7, 10, 18, 19, 37). In the immune system, binding of formylmethionylleucylphenylalanine (f-Met-Leu-Phe) to neutrophil membrane receptors similarly induces immediate increases in ruffling,

pinocytosis, and spreading (11). Furthermore, an increased association of actin with detergent-extracted cell matrices, commonly called cytoskeletons, has been observed after binding of a variety of other ligands to target cells. These include concanavalin A-treated *Dictyostelium discoideum* (9), anti-Ig–treated B lymphocytes (5), neutrophils incubated with concanavalin A and chemotactic peptides (22, 42, 47), and thrombin-treated platelets (36). Thus the same series of cytoskeletal and membrane responses may modulate specific responses to ligand binding in a wide range of target cells.

We thank Dr. H. Metzger for helpful discussion as well as generous assistance with reagents. We also thank Drs. J. Martin and J. Steinkamp (National Flow Cytometry Resource, Los Alamos, NM) for their assistance with the collection of flow cytometry data and Drs. Martin and J. Jett (National Flow Cytometry Resource) for help with data analysis.

This work was supported in part by grant BC-179 from the American Cancer Society, grant 1649 from the Council for Tobacco Research, and National Institutes of Health grant CA 36646.

Received for publication 15 October 1984, and in revised form 16 August 1985.

REFERENCES

1. Baird, B., A. K. Menon, D. Robertson, W. W. Webb, and D. Holowka. 1985. Cell surface cross-linking of IgE-receptor complexes to aggregates larger than dimers results in rapid immobilization and anchoring to a detergent-insoluble cytoskeleton. *Fed. Proc.* 44:1918a. (Abstr.)
2. Beaven, M. A., J. Rogers, J. P. Moore, T. R. Hesketh, G. A. Smith, and J. C. Metcalfe. 1984. The mechanism of the calcium signal and correlation with histamine release in 2H3 cells. *J. Biol. Chem.* 259:7129–7136.
3. Beaven, M. A., J. P. Moore, G. A. Smith, T. R. Hesketh, and J. C. Metcalfe. 1984. The calcium signal and phosphatidylinositol breakdown in 2H3 cells. *J. Biol. Chem.* 259:7137–7142.
4. Becker, E. L. 1972. The relationship of the chemotactic behavior of the complement-derived factors, C3A, C5A, and C567, and a bacterial chemotactic factor to their ability to activate the proesterase of rabbit polymorphonuclear leukocytes. *J. Exp. Med.* 135:376–387.
5. Braun, J., P. S. Hochman, and E. R. Unanue. 1982. Ligand-induced association of surface immunoglobulin with the detergent-insoluble cytoskeletal matrix of the B lymphocyte. *J. Immunol.* 128:1198–1204.
6. Carson, D., and H. Metzger. 1974. Interaction of IgE with rat basophil leukemia cells. IV. Antibody-induced redistribution of IgE receptors. *J. Immunol.* 113:1271–1277.
7. Chinkers, M., J. A. McKanna, and S. Cohen. 1979. Rapid induction of morphological changes in human carcinoma cells A-431 by epidermal growth factor. *J. Cell Biol.* 83:260–265.
8. Cockcroft, S., and B. D. Gomperts. 1983. Role of guanine nucleotide binding protein in the activation of polyphosphoinositol phosphodiesterase. *Nature (Lond.).* 314:534–536.
9. Condeelis, J. 1979. Isolation of concanavalin A caps during various stages of formation and their association with actin and myosin. *J. Cell Biol.* 80:751–758.
10. Connolly, J. L., S. A. Green, and L. A. Greene. 1981. Pit formation and rapid changes in surface morphology of sympathetic neurones in response to nerve growth factor. *J. Cell Biol.* 90:176–180.
11. Davis, B. H., R. J. Walter, C. B. Pearson, E. L. Becker, and J. M. Oliver. 1982. Membrane activity and topography of f-Met-Leu-Phe-treated polymorphonuclear leukocytes. Acute and sustained responses to chemotactic peptide. *Am. J. Pathol.* 108:206–216.
12. Davis, B. H., JC. Seagrave, and J. M. Oliver. 1985. F-actin level changes associated with IgE-mediated stimulation in rat basophil leukemia cells. *Fed. Proc.* 44:1323.
13. Dvorak, A. M., S. J. Galli, E. S. Schulman, L. M. Lichtenstein, and H. F. Dvorak. 1983. Basophil and mast cell degranulation: ultrastructural analysis of mechanism of mediator release. *Fed. Proc.* 42:2510–2515.
14. Fewtrell, C., and H. Metzger. 1980. Larger oligomers of IgE are more effective than dimers in stimulating rat basophilic leukemia cells. *J. Immunol.* 125:701–710.
15. Fewtrell, C., D. Lagunoff, and H. Metzger. 1981. Secretion from rat basophilic leukemia cells induced by calcium ionophores. Effect of pH and metabolic inhibition. *Biochim. Biophys. Acta.* 644:363–368.
16. Frens, G. 1973. Controlled nucleation for regulation of particle size in monodisperse gold suspensions. *Nature Phys. Sci.* 241:20–22.
17. Furuichi, K., J. Rivera, and C. Isersky. 1984. The fate of IgE bound to rat basophilic leukemia cells. III. Relationship between antigen-induced endocytosis and serotonin release. *J. Immunol.* 133:1513–1520.
18. Goshima, K., A. Masuda, and K. Owaribe. 1984. Insulin-induced formation of ruffling membrane of KB cells and its correlation with enhancement of amino acid transport. *J. Cell Biol.* 98:801–809.
19. Haigler, H. T., J. A. McKanna, and S. Cohen. 1979. Rapid stimulation of pinocytosis in human carcinoma cells A-431 by epidermal growth factor. *J. Cell Biol.* 83:82–90.
20. Heiman, A.S., and F. T. Crews. 1985. Characterization of the effects of phorbol esters on rat mast cell secretion. *J. Immunol.* 134:548–555.
21. Holowka, D., H. Hartmann, J. Kanellopoulos, and H. Metzger. 1980. Association of the receptor for immunoglobulin E with endogenous polypeptide on rat basophilic leukemia cells. *J. Recept. Res.* 1:41–68.
22. Howard, J. H., and W. H. Meyer. 1984. Chemotactic peptide modulation of actin assembly and locomotion in neutrophils. *J. Cell Biol.* 98:1265–1271.
23. Isersky, C., J. Rivera, D. M. Segal, and T. Triche. 1983. The fate of IgE bound to rat basophilic leukemia cells. II. Endocytosis of IgE oligomers and effect on receptor turnover. *J. Immunol.* 131:388–396.
24. Jesaitis, A. J., J. R. Naemura, L. A. Sklar, C. G. Cochrane, and R. G. Painter. 1984. Rapid modulation of N-formyl chemotactic peptide receptors on the surface of human granulocytes: formation of high affinity ligand-receptor complexes in transient association with cell cytoskeleton. *J. Cell Biol.* 98:1378–1387.
25. Kanner, B. J., and H. Metzger. 1983. Crosslinking of the receptors for immunoglobulin E depolarizes the plasma membrane of rat basophilic leukemia cells. *Proc. Natl. Acad. Sci. USA.* 80:5744–5748.
26. Laemmli, U. K. 1970. Cleavage of structural proteins during the assembly of the head of bacteriophage T_4. *Nature (Lond.).* 277:680–685.
27. Liu, F-T., J. W. Bohn, E. L. Ferry, H. Yamamoto, C. A. Molinaro, L. A. Sherman, N. R. Klinman, and D. H. Katz. 1980. Monoclonal dinitrophenyl-specific murine IgE antibody preparation, isolation and characterization. *J. Immunol.* 124:2728–2736.
28. Martin, J. C., and D. E. Swartzendruber. 1980. Time: a new parameter for kinetic measurements in flow cytometry. *Science (Wash. DC).* 207:199–201.
29. McCloskey, M. A., Z-Y. Liu, and M-M. Poo. 1984. Lateral electromigration and diffusion of Fc receptors on rat basophilic leukemia cells: effects of IgE binding. *J. Cell Biol.* 99:778–787.
30. Mendoza, G., and H. Metzger. 1976. Distribution and valency of receptor for IgE on rodent mast cells and related tumour cells. *Nature (Lond.).* 264:548–550.
31. Menon, A. K., D. Holowka, and B. Baird. 1984. Small oligomers of immunoglobulin E (IgE) cause large-scale clustering of IgE receptors on the surface of rat basophilic leukemia cells. *J. Cell Biol.* 98:577–583.
32. Nishizuka, Y. 1984. The role of protein kinase C in cell surface signal transduction and tumor promotion. *Nature (Lond.).* 308:693–698.
33. Oliver, J. M., R. D. Berlin, and B. H. Davis. 1984. Use of horseradish peroxidase and fluorescent dextrans to study fluid pinocytosis in leukocytes. *Methods Enzymol.* 108:613–616.
34. Oliver, J. M., JC. Seagrave, J. R. Pfeiffer, M. L. Feibig, and G. G. Deanin. 1985. Surface functions during mitosis in rat basophilic leukemia cells. *J. Cell Biol.* 101:2156–2166.
35. Pfeiffer, J. R., B. H. Davis, G. G. Deanin, and J. M. Oliver. 1984. Surface and cytoskeletal changes associated with IgE-mediated degranulation in rat basophil leukemia cells. *J. Cell Biol.* 99(4, Pt. 2):331a. (Abstr.)
36. Phillips, D. R., L. K. Jennings, and H. H. Edwards. 1980. Identification of membrane proteins mediating the interaction of human platelets. *J. Cell Biol.* 86:77–86.
37. Preston, S. F., R. D. Berlin, and J. M. Oliver. 1983. Immediate effects of MSH on melanoma cells in culture. *J. Cell Biol.* 95(2, Pt. 2):195a. (Abstr.)
38. Ranadive, N. S. 1978. Histamine release from mast cells and basophils. *In* Inflammation. Immunity and Hypersensitivity. H. Z. Movat, editor. Harper and Row. 375–409.
39. Rivnay, B., S. A. Wank, G. Pay, and H. Metzger. 1982. Phospholipids stabilize the interaction between the α and β subunits of the solubilized receptor for immunoglobulin E. *Biochemistry.* 21:6922–6927.
40. Salzmann, G. C., S. F. Wilkins, and J. A. Whitfill. 1981. Modular computer programs for flow cytometry and sorting: the LACEL system. *Cytometry.* 1:325–331.
41. Schecter, Y., K-Y. Chang, S. Jacobs, and P. Cuatrecasas. 1979. Modulation of binding and bioactivity of insulin by anti-insulin antibody: relation to possible role of receptor self aggregation in hormone action. *Proc. Natl. Acad. Sci. USA.* 76:2720–2724.
42. Sheterline, P., and C. R. Hopkins. 1981. Transmembrane linkage between surface glycoproteins and components of the cytoplasm in neutrophil leukocytes. *J. Cell Biol.* 90:743–754.
43. Siraganian, R. P., A. McGivney, E. L. Barsumian, F. T. Crews, F. Hirata, and J. Axelrod. 1982. Variants of the rat basophil leukemia cell line for the study of histamine release. *Fed. Proc.* 41:30–34.
44. Steinkamp, J. 1984. Flow cytometry. *Rev. Sci. Instrum.* 55:1375–1400.
45. Taurog, J. D., G. R. Mendoza, W. A. Hook, R. P. Siraganian, and H. Metzger. 1977. Non-cytotoxic IgE-mediated release of histamine and serotonin from murine mastocytoma cells. *J. Immunol.* 119:1757–1761.
46. Vale, R. D., and E. M. Shooter. 1982. Alteration of binding properties and cytoskeletal attachment of nerve growth factor receptors in PC12 cells by wheat germ agglutinin. *J. Cell Biol.* 94:710–717.
47. Wallace, P. J., R. P. Wersto, C. H. Packman, and M. A. Lichtman. 1984. Chemotactic peptide-induced changes in neutrophil actin conformation. *J. Cell Biol.* 99:1060–1065.
48. Woda, B. A., and M. B. Woodin. 1984. The interaction of lymphocyte membrane proteins with the lymphocyte cytoskeletal matrix. *J. Immunol.* 133:2767–2772.